Transactions of the Korean Nuclear Society Autumn Meeting
Gyeongju, Korea, October 29-30, 2015

Development of OKMC perturbation algorithm for sensitivity analysis of irradiation damage calculation

Yong Hee Choi, Hyung Jin Shim*
Nuclear Eng. Dept., Seoul National University, 1 Gwanak-ro, Gwanak-gu, Seoul 151-744, Korea
Corresponding author: shimhj@snu.ac.kr

1. Introduction

The degradation of structural materials caused by irradiation damage in nuclear facilities is well known phenomenon.[1-4] The normal lattice structure is destroyed through the collision between an irradiation particle and target atom. Then, it creates defects in the matrix depending on the kinetic energy of the recoil atom. On the other hand, those primary defects migrate over a long period of time so that they develop into a large size of defect clusters such as void or dislocation loop. Since the damage process happens in the miscroscopic and macroscopic scale together, it is called as a multiscale phenomenon.

The Object Kinetic Monte Carlo (OKMC) is a calculation method that locates at the middle position of these two different time scales.[5] In the damage calculation, the primary defects are calculated by a short term calculation method such as molecular dynamics where the time scale is order of picoseconds. Then, OKMC extends its time scale up to days, months or years. The results of OKMC such as the average size of defect clusters can also be used to estimate the macroscopic material property change such as yield strength increase based on dislocation theory.

The calculation procedure of OKMC consists of four steps. At the first step, the modeling of the defect is introduced such that the complicated configuration is replaced by a simple geometric object. In most of cases, the shape of object that stands for the strain field formed around the defect are simply assumed to be sphere.[5] The size of strain field depends on the type of defects. The second step is to determine the reaction model among objects. Third step is to determine the physical properties of the objects. The final step of calculation is to apply kinetic Monte Carlo algorithm.

Unfortunately, it's not easy to obtain the background data of the objects for the OKMC calculation in either way from experiments or computational methods. The first principle calculation is considered as a most reliable way of data production for the activation energies for the damage process. However, it's known that the computational cost of the first principle calculation is very expensive in terms of the time and resources.

In the point of efficient data production, the sensitivity of data is an important key. Since each of defect is simplified as an object in OKMC calculations, it inevitably involves so many different kinds of objects and related data. Due to high cost of data production, it's not efficient way to make an effort to produce all data with equal precision. When the data has high sensitivity on the final results, the efforts to reduce uncertainties in the data ensure the better results. If not, it can be a waste of time.

The easiest way to perform the sensitivity analysis is to run each case separately by changing input data, which is known by so called direct subtraction method. Then, the difference in results caused by uncertainties in the input data can be obtained. When the number of data is huge, it is not an economic way of test. The perturbation technique in Monte Carlo calculation provides a more powerful and efficient method for data sensitivity analysis.

The mathematical formulation for Kinetic Monte Carlo (KMC) is derived in [6] and it provides the perturbation technique algorithm based on the differential operator sampling (DOS) method. In this paper, a similar formulation work will be given for the OKMC. Then, another Monte Carlo perturbation technique based on the correlated sampling method (CSM) will be derived from the formulation.

2. Derivation of OKMC Perturbation Formulations

2.1 Mathematical Derivation of OKMC Algorithm

The state of the system is defined by the state vector whose elements are the positions of each object:

$$\mathbf{X} \equiv (\cdots, x_{\alpha,i}, y_{\alpha,i}, z_{\alpha,i}, \cdots), \tag{1}$$

where $x_{\alpha,i}$ represents the x coordinate of i-th object with α type. To perform the sampling of the system state in OKMC, the state vector $\mathbf{X}$ as well as time t are regarded as a random variables. Then, it's possible to sampling the state of the system $\mathbf{X}$ and time t when the joint probability density function for $\mathbf{X}$ and t is available,

Fithorn and Weinberg [7] derived the balance equation for the joint probability density function for $\mathbf{X}$ and t which is given by

$$\frac{\partial P(\mathbf{X},t)}{\partial t} + k(\mathbf{X}) \cdot p(\mathbf{X},t) = S(\mathbf{X},t), \tag{2}$$

$$k(\mathbf{X}) = \int_{\Gamma_{\mathbf{X}\to\mathbf{X}'}} d\mathbf{X}' \cdot k(\mathbf{X} \to \mathbf{X}'), \tag{3}$$

$$S(\mathbf{X},t)=\int_{\Gamma_{\mathbf{X}'\to\mathbf{X}}} d\mathbf{X}'\cdot k(\mathbf{X}'\to\mathbf{X})P(\mathbf{X}',t). \quad (4)$$

$P(\mathbf{X},t)$ represents the joint probability density function for $\mathbf{X}$ and t. $k(\mathbf{X}'\to\mathbf{X})$ denotes the probability per unit time that the system changes from $\mathbf{X}'$ to $\mathbf{X}$. An initial condition at $t=0$ is given by

$$Q(\mathbf{X})\equiv P(\mathbf{X},0)\,. \quad (5)$$

Then, the solution of Eq. (2) with the initial condition of Eq. (5) can be expressed by

$$P(\mathbf{X},t)=e^{-k(\mathbf{X})\cdot t}Q(\mathbf{X})+\int_0^t e^{-k(\mathbf{X})\cdot(t-t')}\cdot S(\mathbf{X},t')dt'. \quad (6)$$

Now let us define the joint transition probability density function for $\mathbf{X}$ and t given by

$$\Psi(\mathbf{X},t)=k(\mathbf{X})\cdot e^{-k(\mathbf{X})\cdot t}\cdot Q(\mathbf{X}) + \int_0^t k(\mathbf{X})\cdot e^{-k(\mathbf{X})\cdot(t-t')}\cdot S(\mathbf{X},t')dt'. \quad (7)$$

By introducing the time-flight kernel, T, and the event kernel, C, defined by

$$T(t'\to t\,|\,\mathbf{X})=k(X)\cdot e^{-k(\mathbf{X})\cdot(t-t')}\,, \quad (8)$$

$$C(\mathbf{X}'\to\mathbf{X})=\frac{k(\mathbf{X}'\to\mathbf{X})}{k(\mathbf{X})}\,, \quad (9)$$

Eq. (7) is rewritten by

$$\Psi(\mathbf{X},t)=\hat{Q}(\mathbf{X},t)+\int_0^t\int_{\Gamma_{\mathbf{X}'\to\mathbf{X}}} K(\mathbf{X}',t'\to\mathbf{X},t)\,\Psi(\mathbf{X}',t')\,, \quad (10)$$

$$\hat{Q}(\mathbf{X},t)=T(0\to t\,|\,\mathbf{X})\,Q(\mathbf{X})\,, \quad (11)$$

$$K(\mathbf{X}',t\to\mathbf{X},t)=T(t'\to t\,|\,\mathbf{X})C(\mathbf{X}'\to\mathbf{X})\,. \quad (12)$$

The solution of Eq. (10) is given by the Neumann series solution given as

$$\Psi(\mathbf{X},t)=\sum_{j=0}^{\infty}\psi_j(\mathbf{X},t), \quad (13)$$

$$\psi_j(\mathbf{X},t)=\int_0^t dt_0\int_{\Gamma_{\mathbf{X}_0}} d\mathbf{X}_0\cdot K_j(\mathbf{X}_0,t_0\to\mathbf{X},t)\hat{Q}(\mathbf{X}_0,t_0)\,, \quad (14)$$

$$\begin{aligned}
&K_0(\mathbf{X}_0,t_0\to\mathbf{X},t)=\delta(\mathbf{X}_0-\mathbf{X})\delta(t_0-t)\,,\\
&K_1(\mathbf{X}_0,t_0\to\mathbf{X},t)=K(\mathbf{X}_0,t_0\to\mathbf{X},t)\,,\\
&\cdots\\
&K_j(\mathbf{X}_0,t_0\to\mathbf{X},t)=\int_{t_{j-2}}^t dt_{j-1}\int_{\Gamma_{\mathbf{X}_{j-1}}} d\mathbf{X}_{j-1}\cdots\int_{t_0}^t dt_1\int_{\Gamma_{\mathbf{X}_1}} d\mathbf{X}_1\\
&\times K(\mathbf{X}_{j-1},t_{j-1}\to\mathbf{X},t)\cdots K(\mathbf{X}_0,t_0\to\mathbf{X}_1,t_1).
\end{aligned} \quad (15)$$

Eq. (13) and (14) shows how to sampling $\mathbf{X}$ and t successively from the joint transition probability density function.

2.2 Correlated sampling method

The expectation value of response function to the successive change of states is given by

$$\langle R\rangle=\int_0^\infty dt\int_{\Gamma_{\mathbf{X}}} d\mathbf{X}\cdot r(\mathbf{X},t)\cdot\Psi(\mathbf{X},t)\,, \quad (16)$$

where $r(\mathbf{X},t)$ is the response at state $\mathbf{X}$ and time t that must be analyzed during the calculation. From Eq. (13) and Eq. (16), it can be shown that the expectation value of response function at the j-th transition step can be written by

$$\langle R\rangle=\sum_{j=0}^{\infty}\langle R_j\rangle\,, \quad (17)$$

and

$$\langle R_j\rangle\equiv\int_{t_{j-1}}^{\infty} dt_j\int_{\Gamma_{\mathbf{X}_j}} d\mathbf{X}_j\; r(\mathbf{X}_j,t_j)\cdot\psi_j(\mathbf{X}_j,t_j). \quad (18)$$

The main concerns in irradiation damage calculation is the time evolution of defects so that the number of objects and time can be taken as the major responses in OKMC. By denoting $N_{\alpha,j}$ be the number of α type objects at the j-th transition step, it can be shown from Eq. (13) and Eq. (18) that the expectation value of the difference in the number of objects between successive states can be expressed by

$$\begin{aligned}
\langle\Delta N_{\alpha,j}\rangle=&\int_{t_{j-2}}^{\infty} dt_j\int_{\Gamma_{\mathbf{X}_j}} d\mathbf{X}_j\cdots\int_0^{\infty} dt_0\int_{\Gamma_{\mathbf{X}_0}} d\mathbf{X}_0\\
&\times\left[N_{\alpha,j}-N_{\alpha,j-1}\right]C(\mathbf{X}_{j-1}\to\mathbf{X}_j)\,T(t_{j-1}\to t_j\,|\,\mathbf{X}_j)\\
&\cdots C(\mathbf{X}_0\to\mathbf{X}_1)\,T(0\to t_0\,|\,\mathbf{X}_0)\,.
\end{aligned} \quad (19)$$

Note that the number of objects is only function of state vector $\mathbf{X}$ so that Eq. (19) can be reduced to

$$\begin{aligned}
\langle\Delta N_{\alpha,j}\rangle=&\int_{\Gamma_{\mathbf{X}_j}} d\mathbf{X}_j\cdots\int_{\Gamma_{\mathbf{X}_0}} d\mathbf{X}_0\left[N_{\alpha,j}-N_{\alpha,j-1}\right]\\
&\times C(\mathbf{X}_{j-1}\to\mathbf{X}_j)\,\Phi(X_{j-1})\,,
\end{aligned} \quad (20)$$

where $\Phi(\mathbf{X})$ denotes the marginal transition probability density function only for state vector $\mathbf{X}$ which can be expressed recursively by

$$\Phi(\mathbf{X}_j)=\begin{cases} Q(\mathbf{X}_0) & j=0\\ \displaystyle\int_{\Gamma_{\mathbf{X}_{j-1}}} d\mathbf{X}_{j-1}\cdot C(\mathbf{X}_{j-1}\to\mathbf{X}_j)\cdot\Phi(\mathbf{X}_{j-1}) & j>0\end{cases}\,. \quad (21)$$

In the same way, the expectation value of the difference in the elapsed time at the j-th transition step, Δt_j, is given by

$$\left\langle \Delta t_j \right\rangle = \int_{t_{j-1}}^{\infty} dt_j \int_{\Gamma_{\mathbf{X}_j}} d\mathbf{X}_j \cdot \Delta t_j \cdot T\left(t_{j-1} \to t_j \mid \mathbf{X}_j\right) \cdot \Phi\left(\mathbf{X}_j\right). \quad (22)$$

Rief [8] proved that the correlation of sampling is one of the possible way to avoid the divergence of relative variance of two different Monte Carlo integrations for the two different systems with a small perturbation. One way of correlating the Monte Carlo integration such as Eq. (20) and Eq. (22) can be given by

$$\begin{aligned} \left\langle \Delta N^*_{\alpha,j} \right\rangle = & \int_{\Gamma_{\mathbf{X}_j}} d\mathbf{X}_j \cdots \int_{\Gamma_{\mathbf{X}_0}} d\mathbf{X}_0 \left[N_{\alpha,j} - N_{\alpha,j-1} \right] \\ & \times u\left(\mathbf{X}_{j-1}, \mathbf{X}_j\right) C\left(\mathbf{X}_{j-1} \to \mathbf{X}_j\right) \Phi^*\left(\mathbf{X}_{j-1}\right), \end{aligned} \quad (23)$$

$$\begin{aligned} \left\langle \Delta t^*_j \right\rangle = & \int_{t_{j-1}}^{\infty} dt_j \int_{\Gamma_{\mathbf{X}_j}} d\mathbf{X}_j \, \Delta t_j \\ & \times w\left(t_{j-1}, t_j \mid \mathbf{X}_j\right) T\left(t_{j-1} \to t_j \mid \mathbf{X}_j\right) \cdot \Phi^*\left(\mathbf{X}_j\right), \end{aligned} \quad (24)$$

where the asterisk denotes the perturbed system and

$$u\left(\mathbf{X}_{j-1}, \mathbf{X}_j\right) \equiv \frac{C^*\left(\mathbf{X}_{j-1} \to \mathbf{X}_j\right)}{C\left(\mathbf{X}_{j-1} \to \mathbf{X}_j\right)}, \quad (25)$$

$$w\left(t_{j-1}, t_j \mid \mathbf{X}_j\right) \equiv \frac{T^*\left(t_{j-1} \to t_j \mid \mathbf{X}_j\right)}{T\left(t_{j-1} \to t_j \mid \mathbf{X}_j\right)}, \quad (26)$$

$$\Phi^*\left(\mathbf{X}_j\right) = \int_{\Gamma_{\mathbf{X}_{j-1}}} d\mathbf{X}_{j-1} \cdot u\left(\mathbf{X}_{j-1}, \mathbf{X}_j\right) \cdot C\left(\mathbf{X}_{j-2} \to \mathbf{X}_{j-1}\right) \cdot \Phi^*\left(\mathbf{X}_{j-1}\right). \quad (27)$$

By introducing the correlated sampling scheme described in Eq. (23)-(27), the variation of the correlation between object numbers and time due to a deviation of input parameter can be examined.

3. Numerical results

The target material is assumed to be pure BCC iron. Table 1 shows the reaction model used in the simulation.

Events	Reactions
SIA aggregation	$I_m + I_{m'} \to I_{m+m'}$
V aggregation	$V_m + V_{m'} \to V_{m+m'}$
Recombination	$I_n + V_m \to \begin{cases} I_{(n-m)} & n > m \\ V_{(m-n)} & n < m \\ \phi & n = m \end{cases}$

Table 1 Possible object reactions: V stands for vacancy and I stands for SIA

For simplicity, it's supposed that the irradiation particle is an electron so that the Frenkel pair are created whenever a collision occurs in the matrix. The number of collision rate is assumed as 2.82e+22 $\#/cm^3 \cdot s$. The size of problem domain is 500*500*500 Angstroms along each side with periodic boundary condition. The temperature is set to 300K. The parameter set given in [5] are used for the migration energy and attempt frequency of the objects summarized in the Table 2.

Object type	Attempt frequency (/sec)	Migration energy (eV)		
		Ref.	Set A	Set B
I1	1.0e+12	0.34	**0.34±0.02**	0.34
I2	4.2e+12	0.34	0.34	**0.34±0.02**
I3	3.4e+12	0.34	0.34	0.34
I4	2.9e+12	0.34	0.34	0.34
I5	2.6e+12	0.34	0.34	0.34
V1	6.0e+12	0.65	0.65	0.65
V2	1.0e+09	0.65	0.65	0.65
V3	1.0e+06	0.65	0.65	0.65
V4	1.0e+03	0.65	0.65	0.65
V5	1.0e+00	0.65	0.65	0.65
others	Immobile			

Table 2 Parameter sets for object migration

On the other hand, the data set A and set B given in Table 2 can be considered as perturbed cases from the reference data set. In the case of data set A, the migration energy of single SIA is only changed by ± 0.02eV from the reference case. In the case of data set B, the migration energy of di-SIA clusters denoted by I2 is only perturbed by the amount of ± 0.02eV. For simplicity, the dissociation of the large clusters is not considered in the simulation.

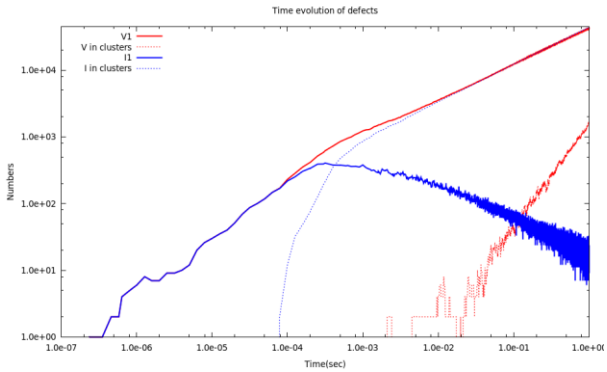

Figure 1 Time evolution of number of defects with reference data set

Fig. 1 shows the time evolution of the number of vacancies and SIAs with the reference data set. At the initial stage, the number of point defects increase linearly with the same numbers. As SIA clusters are formed at about 1e-4s, it's observed that the number of single SIA start to decrease. Fig. 2 shows the time

evolution of the number of various sizes of SIA clusters. It shows the time evolution of SIA clusters happens in the order of cluster sizes. It makes sense that the increase of number of clusters is only followed after increasing the number of smaller size clusters. Since the single SIA shows the largest variation in time among all objects, it can be considered as a good target of sensitivity analysis to the data uncertainties.

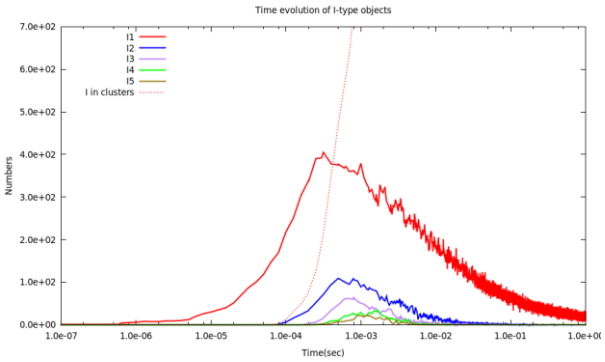

Figure 2 Time evolution of number of various size of SIA clusters with reference data set

Fig. 3 shows the results obtained with the data set A in Table 2. The difference in data set A and reference data set lies only in the migration energy of single SIA so that it can be considered that the result stands for the sensitivity of the time evolution of single SIA number to the migration energy of single SIA. Fig. 3 shows that the sensitivity of the number of single SIA is very large to the migration energy of single SIA. A small variation of input data induces a different path of time evolution for the single SIA.

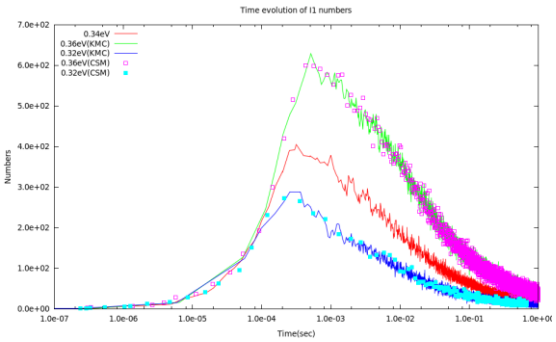

Figure 3 Time evolution of single SIA with the reference data set and data set A. The real line stands for the independent run of OKMC, while the dotted lines are results obtained by perturbation calculation

On the other hand, the results denoted by the real line in Fig. 3 is obtained by direct running of the case, while the dots are the one obtained from the perturbation calculation. It shows that two results are in good agreements.

Fig. 4 shows the time evolution of di-SIA clusters for the reference data set and set A. It shows the sensitivity of di-SIA cluster is lower than single SIA to the migration energy of single SIA so that the results are not so different for each case. It also shows that the perturbation calculation works well even in this case where the sensitivity to the data is low.

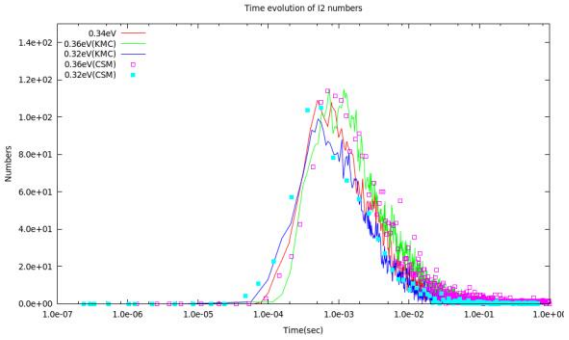

Figure 4 Time evolution of di-SIA clusters with reference data set and set A

Fig. 5 shows the comparison of the time evolution of the number of single SIA with the reference data set and data set B. It shows the uncertainties in the migration energy for di-SIA has no effect on the behavior of single SIA, whereas it affects significantly to the behavior of di-SIA clusters as shown in Fig. 6. In this case, it also reveals that the perturbation calculation works very well so that the results are same in the case where the OKMC runs directly.

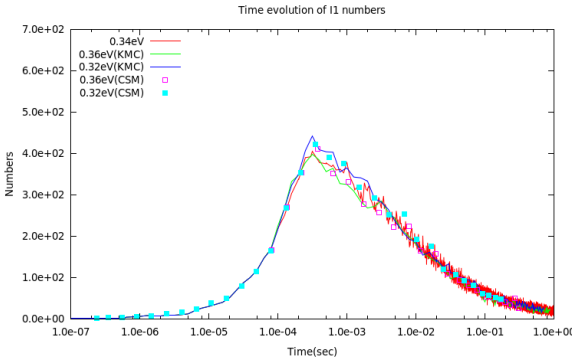

Figure 5 Time evolution of single SIA with the reference data set and data set B

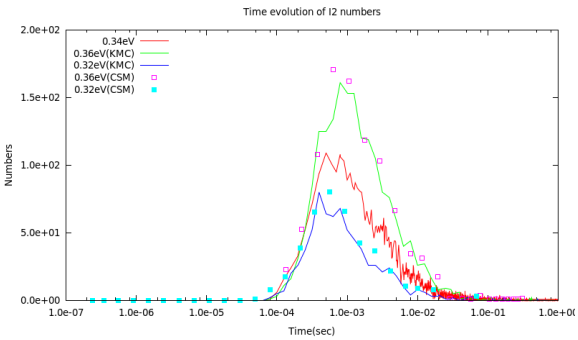

Figure 6 Time evolution of di-SIA clusters with the reference data set and data set B

4. Conclusion

We have derived an OKMC algorithm mathematically and developed an OKMC perturbation algorithm newly based on correlated sampling method. The developed algorithm has been applied to the test problem where the target is pure BCC iron and irradiated particle is electron. The results shows that the perturbation algorithm works well so that it can be used in the prediction of sensitivity.

REFERENCES

[1] L.R. Greenwood, Neutron interactions and atomic recoil spectra, J. Nucl. Mater. 216 (1994) 29–44.
[2] H. Fukushima, Y. Shimomura, et al., Dependence of Observed Cascade Defects on Neutron Spectrum and Dose in Au and Ag Irradiated with Fission and Fusion Neutrons at Low Temperature, J. Nucl. Mater. 212–215 (Part 1) (1994) 154–159.
[3] R.E. Stoller, The Effect of Neutron Flux on Radiation-Induced Embrittlement in Reactor Pressure Vessel Steels, J. Test. Eval. International 1 (4) (2004) 326–336.
[4] H.L. Heinisch, S.D. Atkin, C. Martinez, Spectral effects in low-dose fission and fusion neutron irradiated metals and alloys, J. Nucl. Mater. 141–143 (Part 2) (1986) 807–815.
[5] C. Domain, C.S. Becquart, L. Malerba, Simulation of Radiation Damage in Fe Alloys: an Object Kinetic Monte Carlo Approach, Journal of Nuclear Materials 335 (1) (2004) 121–145.
[6] Hyung Jin Shim, Kinetic Monte Carlo Perturbation analysis for adsorption dynamics, Trans. Korean Nuclear Society Spring Meeting, Gwangju, Korea, (2013).
[7] Fithorn and Weinberg, Theoretical Foundations of Dynamical Monte Carlo Simulations, J. Chem. Phys., 95, 2, 1090, 1991.
[8] Herbert Rief, A Symopsis of Monte Carlo Perturbation Algorithms, Journal of Computational Physics 111, 33-48 (1994).